Eur. Phys. J. A **29**, 23–26 (2006)
DOI 10.1140/epja/i2005-10292-x

THE EUROPEAN
PHYSICAL JOURNAL A

NeXSPheRIO results on elliptic flow at RHIC and connection with thermalization

R. Andrade[1], F. Grassi[1,a], Y. Hama[1], T. Kodama[2], O. Socolowski jr.[3], and B. Tavares[2]

[1] Instituto de Física, USP, C. P. 66318, 05315-970 São Paulo-SP, Brazil
[2] Instituto de Física, UFRJ, C. P. 68528, 21945-970 Rio de Janeiro-RJ, Brazil
[3] CTA/ITA, Praça Marechal Eduardo Gomes 50, CEP 12228-900 São José dos Campos-SP, Brazil

Received: 11 November 2005 /

Abstract. Elliptic flow at RHIC is computed event by event with NeXSPheRIO. Reasonable agreement with experimental results on $v_2(\eta)$ is obtained. Various effects are studied as well: reconstruction of impact parameter direction, freeze-out temperature, equation of state (with or without crossover), emission mechanism.

PACS. 24.10.Nz Hydrodynamic models – 25.75.Ld Collective flow – 25.75.-q Relativistic heavy-ion collisions

1 Motivation

Hydrodynamics seems a correct tool to describe RHIC collisions, however, $v_2(\eta)$ is not well reproduced as shown by Hirano *et al.* [1]. These anthors suggested that this might be due to lack of thermalization. Heinz and Kolb [2] presented a model with partial thermalization and obtained a reasonable agreement with data. The question addressed in this work is whether lack of thermalization is the only explaination for this disagreement between data and theory for $v_2(\eta)$.

2 Brief description of NeXSPheRIO

The tool we use is the hydrodynamical code called NeXSPheRIO. It is a junction of two codes.

The SPheRIO code is used to compute the hydrodynamical evolution. It is based on Smoothed Particle Hydrodynamics, a method originally developped in astrophysics and adapted to relativistic heavy-ion collisions [3]. Its main advantage is that any geometry in the initial conditions can be incorporated.

The NeXus code is used to compute the initial conditions $T_{\mu\nu}$, j^μ and u^μ on a proper time hypersurface [4]. An example of initial condition for one event is shown in fig. 1.

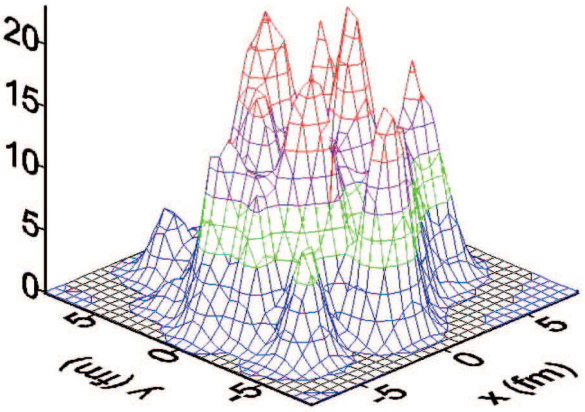

Fig. 1. Example of initial energy density in the $\eta = 0$ plane.

NeXSPheRIO is run many times, corresponding to many different events or initial conditions. In the end, an average over final results is performed. This mimicks experimental conditions. This is different from the canonical approach in hydrodynamics where initial conditions are adjusted to reproduce some selected data and are very smooth.

This code has been used to study a range of problems concerning relativistic nuclear collisions: effect of fluctuating initial conditions on particle distributions [5], energy dependence of the kaon effective temperature [6], interferometry at RHIC [7], transverse mass ditributions at SPS for strange and non-strange particles [8].

3 Results

3.1 Theoretical vs. experimental computation

Theoretically, the impact parameter angle ϕ_b is known and varies in the range of the centrality window chosen. The

---

[a] e-mail: `grassi@if.usp.br`

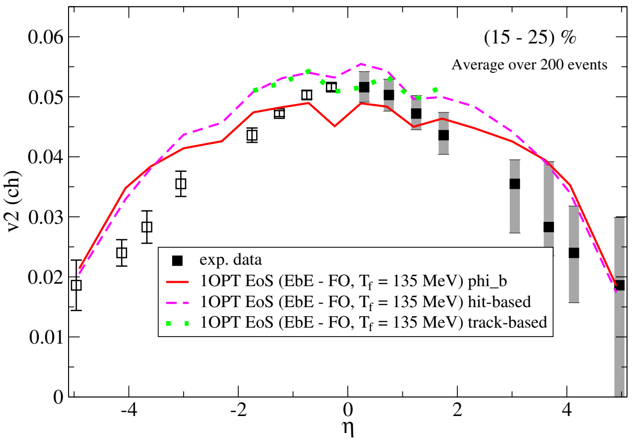

Fig. 2. Comparison of various ways of computing v_2: the solid line is obtained using the known impact parameter angle ϕ_b, the dashed and dotted lines are obtained using the reconstructed impact parameter angle ψ_2. 1OPT stands for equation of state with first-order transition, EbE, event-by-event calculation, FO, freeze-out mechanism for particle emission. Data are from Phobos [9]. For more details see text.

elliptic flow can be computed easily through

$$\langle v_2^b(\eta)\rangle = \left\langle \frac{\int \mathrm{d}^2N/\mathrm{d}\phi\,\mathrm{d}\eta \cos[2(\phi-\phi_b)]\,\mathrm{d}\phi}{\int \mathrm{d}^2N/\mathrm{d}\phi\,\mathrm{d}\eta\,\mathrm{d}\phi} \right\rangle . \qquad (1)$$

The average is performed over all events in the centrality bin. This is shown by the lowest solid curve in fig. 2.

Experimentally, the impact parameter angle ψ_2 is reconstructed and a correction is applied to the elliptic flow computed with respect to this angle, to correct for the reaction plane resolution. For example in a Phobos-like way [9]

$$\langle v_2^{b,rec}(\eta)\rangle = \left\langle \frac{v_2^{obs}(\eta)}{\sqrt{\langle \cos[2(\psi_2^{<0}-\psi_2^{>0})]\rangle}} \right\rangle , \qquad (2)$$

where

$$v_2^{obs}(\eta) = \frac{\sum_i \mathrm{d}^2N/\mathrm{d}\phi_i\mathrm{d}\eta \cos[2(\phi_i-\psi_2)]}{\sum_i \mathrm{d}^2N/\mathrm{d}\phi_i\mathrm{d}\eta} \qquad (3)$$

and

$$\psi_2 = \frac{1}{2}\tan^{-1}\frac{\sum_i \sin 2\phi_i}{\sum_i \cos 2\phi_i} . \qquad (4)$$

In the hit-based method, $\psi_2^{<0}$ and $\psi_2^{>0}$ are determined for subevents $\eta<0$ and >0, respectively, and if v_2 is computed for a positive (negative) η, the sum in ψ_2, eq. (3), is over particles with $\eta<0$ ($\eta>0$).

In the track-based method, $\psi_2^{<0}$ and $\psi_2^{>0}$ are determined for subevents $2.05 <| \eta |< 3.2$ and v_2 is obtained for particles around $0<\eta<1.8$ and reflected (there is also an additional $\sqrt{2}$ in the reaction plane correction in eq. (2)).

In fig. 2, we also show the results for $v_2^{obs}(\eta)$ for both the hit-based (dashed line) and track-based (dotted line) methods. We see that both curves can lie *above* the theoretical $\langle v_2^b(\eta)\rangle$ (solid) curve. So dividing them by a cosine to get $\langle v_2^{b,rec}(\eta)\rangle$ will make the disagreement worse: $\langle v_2^b(\eta)\rangle$ and $\langle v_2^{b,rec}(\eta)\rangle$ are different.

Since the standard way to include the correction for the reaction plane resolution (eq. (2)) seems inapplicable, we need to understand why. When we look at the distribution $\mathrm{d}^2N/\mathrm{d}\phi\mathrm{d}\eta$ obtained with NeXSPheRIO, it is not symmetric with respect to the reaction plane. This happens because the number of produced particles is finite. Therefore, we must write

$$\begin{aligned}\frac{\mathrm{d}^2N}{\mathrm{d}\phi\,\mathrm{d}\eta} &= v_0^b(\eta)\Big[1+\sum 2v_n^b(\eta)\cos(n(\phi-\phi_b)) \\ &\quad +\sum 2v_n^{\prime b}(\eta)\sin(n(\phi-\phi_b))\Big] \qquad (5)\\ &= v_0^b(\eta)\Big[1+\sum 2v_n^{obs}(\eta)\cos(n(\phi-\psi_2)) \\ &\quad +\sum 2v_n^{\prime obs}(\eta)\sin(n(\phi-\psi_2))\Big]. \qquad (6)\end{aligned}$$

It follows that

$$v_2^{obs}(\eta) = v_2^b(\eta)\cos[2(\psi_2-\phi_b)]+v_2^{\prime b}(\eta)\sin[2(\psi_2-\phi_b)]. \quad (7)$$

We see that due to the term in sine, we can indeed have $\langle v_2^{obs}(\eta)\rangle$ larger than $\langle v_2^b(\eta)\rangle$, as in fig. 2. (The sine term does not vanish upon averaging on events because if a choice such as eq. (4) is done for ψ_2, $v_2^{\prime b}(\eta)$ and $\sin(2(\psi_2-\phi_b))$ have same sign. Rigorously, this sign condition is true if ψ_2 is computed for the same η as $v_2^{\prime b}(\eta)$. Due to the actual way of extracting ψ_2 experimentally, we expect this condition is satisfied for particles with small or moderate pseudorapidity.) In the standard approach, it is supposed that $\mathrm{d}^2N/\mathrm{d}\phi\mathrm{d}\eta$ is symmetric with respect to the reaction plane and there are no sine terms in the Fourier decomposition of $\mathrm{d}^2N/\mathrm{d}\phi\mathrm{d}\eta$ (eq. (5)); as a consequence, $v_2^{obs}(\eta) \le v_2^b(\eta)$.

Since the experimental results for elliptic flow are obtained assuming that $\mathrm{d}^2N/\mathrm{d}\phi\mathrm{d}\eta$ is symmetric around the reaction plane, we cannot expect perfect agreement of our $\langle v_2^b(\eta)\rangle$ with them. In the following we use the theoretical method, *i.e.* $\langle v_2^b(\eta)\rangle$, to make further comparisons.

3.2 Study of various effects which can influence the shape of $v_2(\eta)$

In all comparisons, the same set of initial conditions is used, scaled to reproduce $\mathrm{d}N/\mathrm{d}\eta$ for $T_{f.out}=135\,\mathrm{MeV}$.

First, we study the effect of the freeze-out temperature on the pseudorapidity and transverse momentum distributions as well as $v_2(\eta)$ (this last quantity is shown in fig. 3). We found that $v_2(\eta)$ and $\mathrm{d}^2N/p_t\,\mathrm{d}p_t$ favor $T_{f.out}=135\,\mathrm{MeV}$, so this temperature is used thereafter.

We now compare results obtained for a quark matter equation of state with first-order transition to hadronic matter and with a crossover (for details see [10]). We have checked that the η and p_t distributions are not much affected. We expect larger v_2 for crossover because there is always acceleration and this is indeed what is seen in fig. 4.

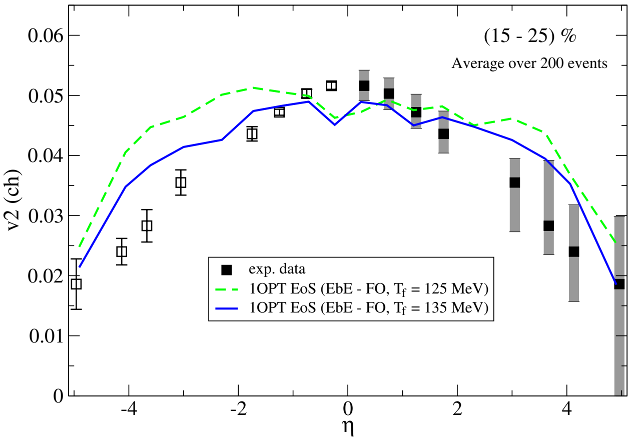

Fig. 3. Comparison of $v_2(\eta)$ for two freeze-out temperatures. Abbreviations: see fig. 2.

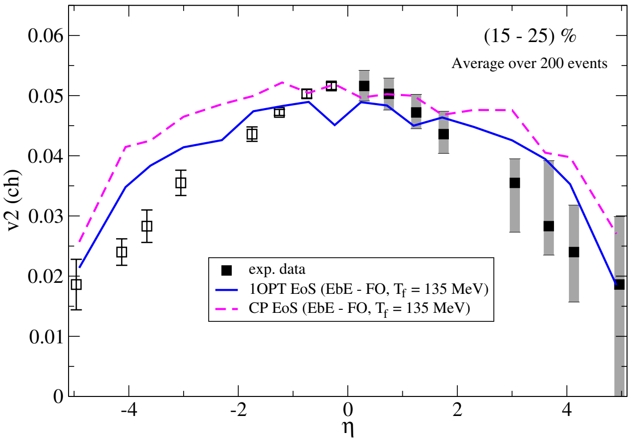

Fig. 4. Comparison of $v_2(\eta)$ for first-order transition (1OPT) and critical point (CP) equations of state.

We then compare results obtained for freeze-out and continuous emission [11]. Again, we have checked that the η and p_t distributions are not much affected. We expect earlier emission, with less flow, at large $|\eta|$ regions, therefore, narrower $v_2(\eta)$ and this is indeed what is seen in fig. 5.

Finally, we note that compared to Hirano's pioneering work with smooth initial conditions, the fact that we used event-by-event initial conditions seems crucial: we immediately avoid the two-bump structure. To check this, it is interesting to study what we would get with smooth initial conditions. We obtained such conditions by averaging the initial conditions of 30 Nexus events. Again, we have checked that the η and p_t distributions are not much affected, but preleminary results shown in fig. 6 indicate that now v_2 is very different, having a bumpy structure. The case of smooth initial conditions has a well-defined asymmetry and the elliptic flow reflects this. The ellipict flow of the event-by-event case is an average over results obtained for randomly varying initial conditions, each with a different asymmetry. As a consequence, the average v_2 has a smoother behavior but large fluctuations [10] and is smaller (around the initial energy density sharp peaks seen in fig. 1, in each event, expansion is more symmetric. No such sharp peak exists for the average initial conditions).

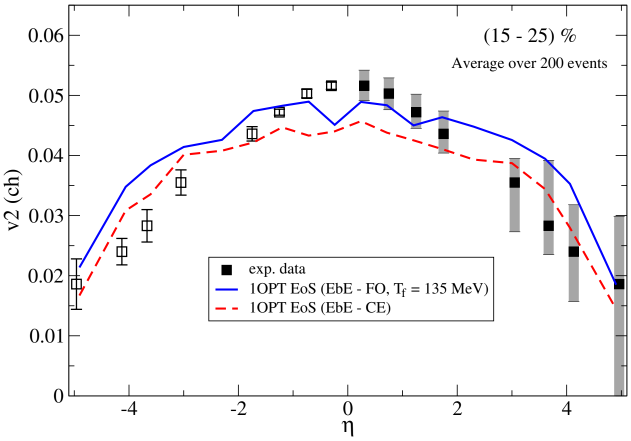

Fig. 5. Comparison of $v_2(\eta)$ for freeze out (FO) and continuous emission (CE).

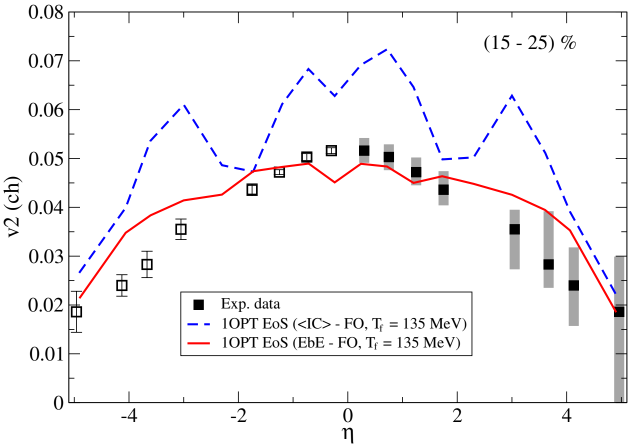

Fig. 6. Comparison of $v_2(\eta)$ computed event by event (EbE) and with smooth initial conditions ($\langle IC \rangle$).

4 Summary

$v_2(\eta)$ was computed with NeXSPheRIO at RHIC energy. Event-by-event initial conditions seem important to get the right shape of $v_2(\eta)$ at RHIC. Other features seem less important: freeze-out temperature, equation of state (with or without crossover), emission mechanism. Finally, we have shown that the reconstruction of the impact parameter direction ψ_2, as given by eq. (4), gives $v_2^{obs}(\eta) > v_2^b(\eta)$, when taking into account the fact that the azimuthal particle distribution is not symmetric with respect to the reaction plane.

Lack of thermalization is not necessary to reproduce $v_2(\eta)$. The fact that there is thermalization outside mid-pseudorapidity is reasonable given that the (averaged) initial energy density is high there (figure not shown). A somewhat similar conclusion was obtained by Hirano (these proceedings), using color glass condensate initial conditions for a hydrodynamical code and emission through a cascade code [12].

We acknowledge financial support by FAPESP (2004/10619-9, 2004/13309-0, 2004/15560-2), CAPES/PROBRAL, CNPq, FAPERJ and PRONEX.

References

1. T. Hirano, Phys. Rev. C **65**, 011901 (2001); T. Hirano, K. Tsuda, Phys. Rev. C **66**, 054905 (2002).
2. U. Heinz, P.F. Kolb, J. Phys. G **30**, S1229 (2004).
3. C.E. Aguiar, T. Kodama, T. Osada, Y. Hama, J. Phys. G **27**, 75 (2001).
4. H.J. Drescher, F.M. Lu, S. Ostapchenko, T. Pierog, K. Werner, Phys. Rev. C **65**, 054902 (2002); Y. Hama, T. Kodama, O. Socolowski jr., Braz. J. Phys. **35**, 24 (2005).
5. C.E. Aguiar, Y. Hama, T. Kodama, T. Osada, Nucl. Phys. A **698**, 639c (2002).
6. M. Gazdzicki, M.I. Gorenstein, F. Grassi, Y. Hama, T. Kodama, O. Socolowski jr., Braz. J. Phys. **34**, 322 (2004); Acta Phys. Pol. B **35**, 179 (2004).
7. O. Socolowski jr., F. Grassi, Y. Hama, T. Kodama, Phys. Rev. Lett. **93**, 182301 (2004).
8. F. Grassi, Y. Hama, T. Kodama, O. Socolowski jr., J. Phys. G **30**, S1041 (2005).
9. B.B. Back, M.D. Baker, D.S. Barton *et al.*, Phys. Rev. Lett. **89**, 222301 (2002); B.B. Back, M.D. Baker, M. Ballintijn *et al.*, Phys. Rev. C **72**, 051901 (2005).
10. Y. Hama, R. Andrade, F. Grassi *et al.*, hep-ph/0510096; hep-ph/0510101.
11. F. Grassi, Y. Hama, T. Kodama, Phys. Lett. B **355**, 9 (1995); Z. Phys. C **73**, 153 (1996).
12. T. Hirano, these proceedings, nucl-th/0510005.